Constraints on Higgs boson properties using WW*(→eνμν)jj final state with the ATLAS detector

Magdalena Sławińska

IFJ PAN

Outline

- SM predictions for the Higgs boson production and branching ratios
- Highlights from the Higgs discovery by ATLAS
- Run 1 measurements in the HWW final state
  - cross-section of ggf and VBF production channels
  - spin and CP properties of the Higgs
- Run 2 studies
  - cross-section of ggf and VBF production channels (run1 and run 2)
  - constraints on anomalous Higgs boson couplings

Disclaimer: I will not present an exhaustive overview of numerous experimental results, but rather focus on selected measurements in the **WW*(→eνμν)jj** final state. I will present ATLAS results only.

The SM predictions for the Higgs boson

Due to the small Higgs boson width, the production and decay can be decoupled.

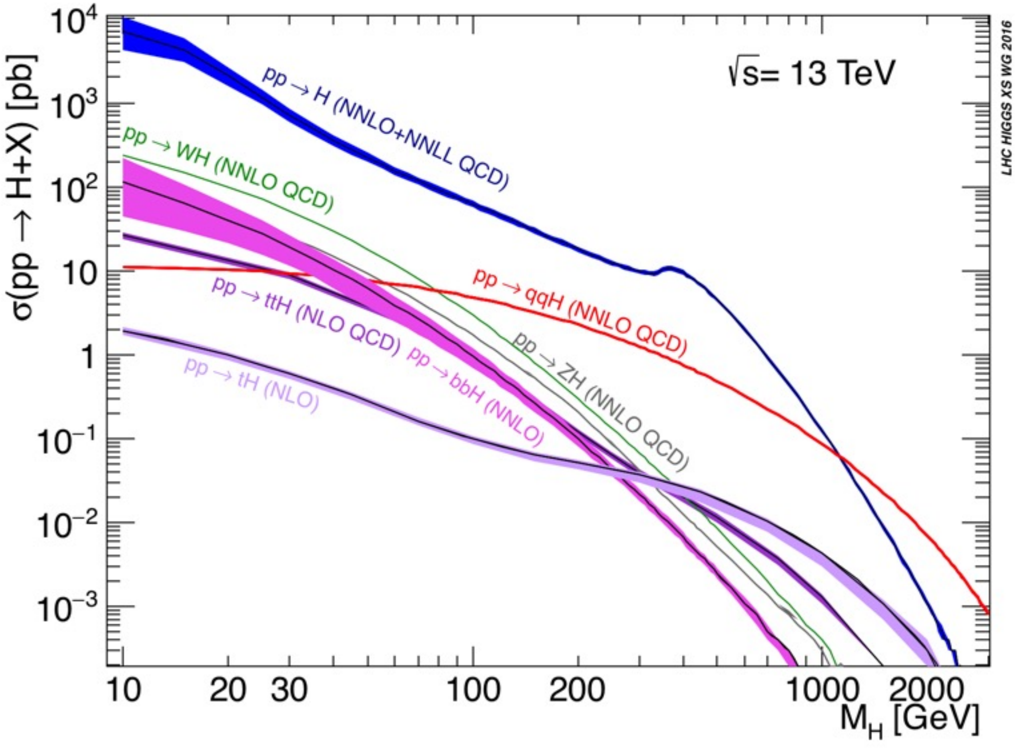

Production cross-sections

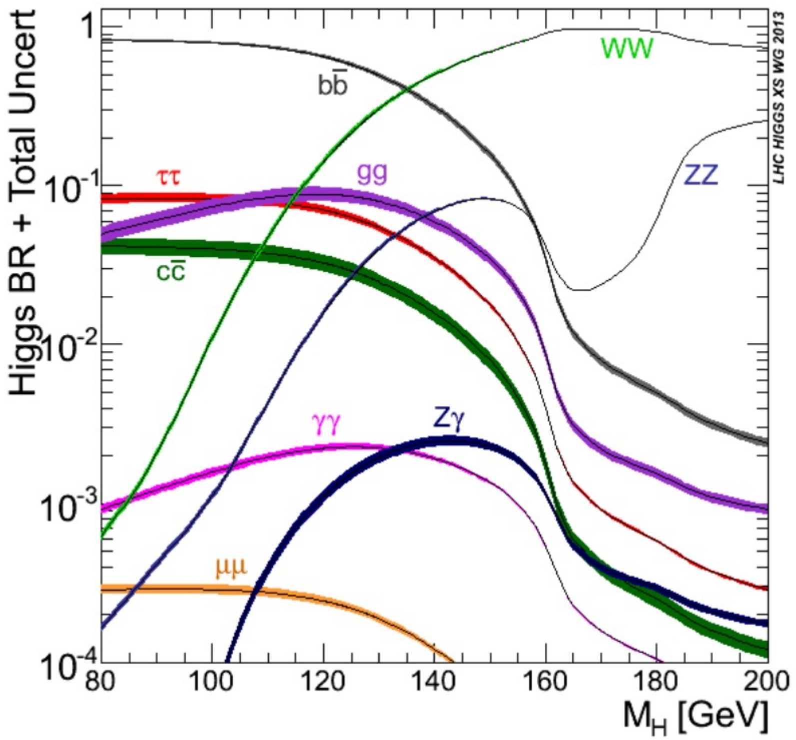

Branching ratios

The SM predictions for the Higgs boson

Due to the small Higgs boson width, the production and decay can be decoupled.

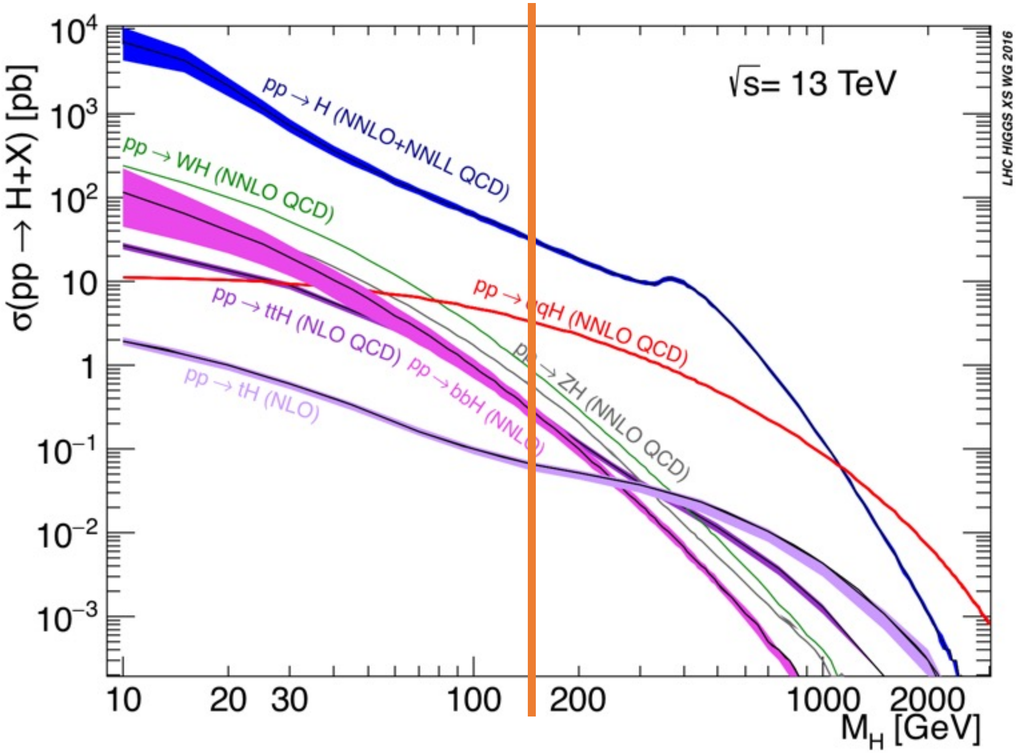

Production cross-sections

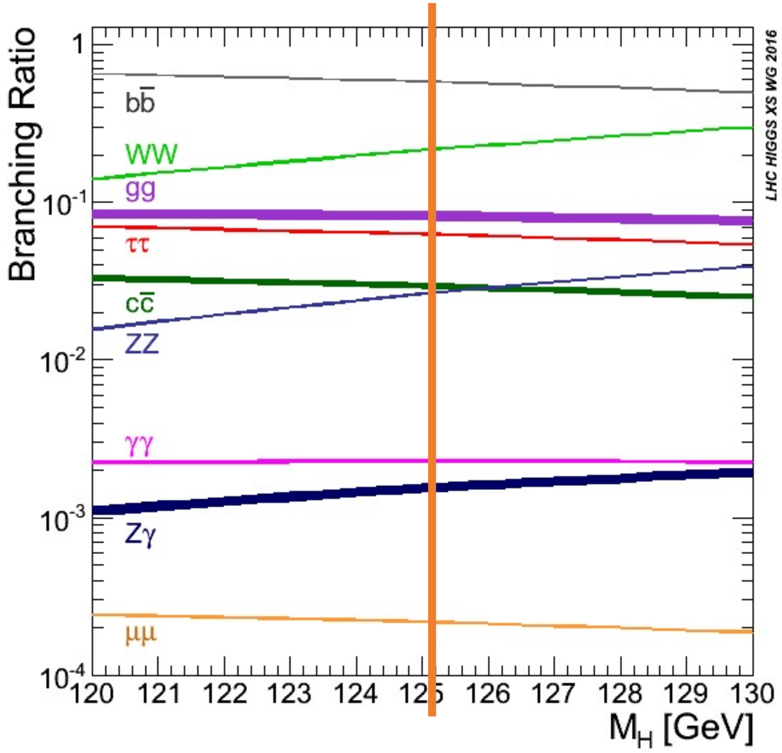

Branching ratios

Phys.Lett. B716 (2012) 1-29

Higgs boson discovery 2012

- based upon integrated luminosities of approximately 4.8 fb^{-1} collected at √s = 7 TeV in 2011 and 5.8 fb^{-1} at √s = 8 TeV in 2012,
- using Higgs decays into H->ZZ*-> 4ℓ, H-> γγ and H->WW->e →$\mu\upsilon e\upsilon$
- Confidence intervals in the (μ, m_H) plane for the 3 channels independently

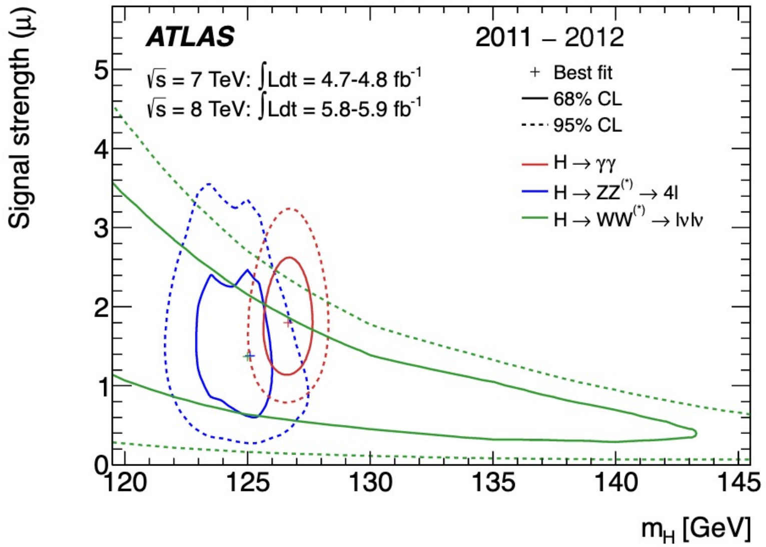

Kinematics of the H→ WW*→eνμν decay

- small invariant mass of dilepton system, m_{ll}.
- small angle between two energetic leptons in the plane perpendicular to the beam, in comparison with leptons originating from non-resonant WW production processes.
- The m_T distribution has a kinematic upper bound at the Higgs boson mass in contrast to non-resonant WW and top quark production

$$m_{\mathrm{T}} = \sqrt{(E_{\ell\ell} + E_{\mathrm{T}}^{miss})^2 - |p_{\mathrm{T},\ell\ell} + E_{\mathrm{T}}^{miss}|^2}$$

Physics Letters B 726 (2013) 88–119
Physics Letters B 726 (2013) 120–144

Couplings to bosons and fermions, spin and parity in Run 1

Cross section (pb) at $\sqrt{s} = 8$ (7) TeV		Branching ratio (relative uncertainty)	
ggF	19.52 (15.32)	$H \to WW^* \to \ell\nu\ell\nu$	0.010 (±5%)
VBF	1.58 (1.22)	$H \to \gamma\gamma$	2.28×10^{-3} (±5%)
WH	0.70 (0.57)	$H \to ZZ^* \to 4\ell$	1.25×10^{-4} (±5%)
ZH	0.39 (0.31)		
$t\bar{t}H$	0.13 (0.09)		
Total	22.32 (17.51)		

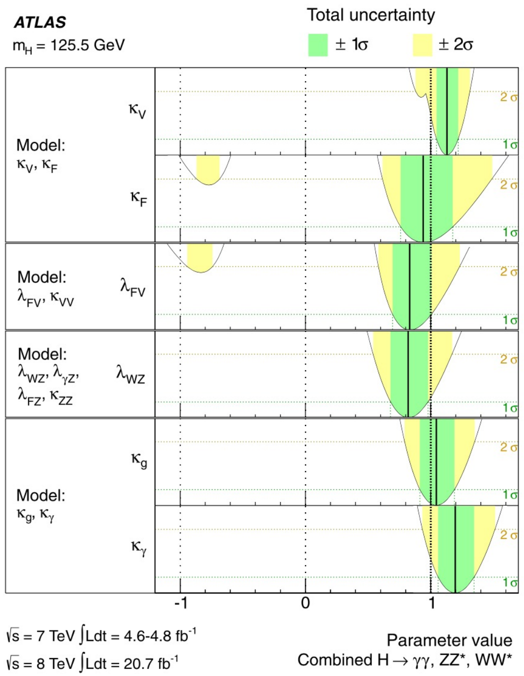

coupling modifications scale factors

- Spin/CP properties established using testing of statistical hypotheses:

Table 1
Summary of results for the 0^+ versus 0^- test in the $H \to ZZ^*$ channel. The expected p_0-values for rejecting the 0^+ and 0^- hypotheses (assuming the alternative hypothesis) are shown in the second and third columns. The fourth and fifth columns show the observed p_0-values, while the $\mathrm{CL_s}$ value for excluding the 0^- hypothesis is given in the last column.

Channel	0^- assumed Exp. $p_0(J^P = 0^+)$	0^+ assumed Exp. $p_0(J^P = 0^-)$	Obs. $p_0(J^P = 0^+)$	Obs. $p_0(J^P = 0^-)$	$\mathrm{CL_s}(J^P = 0^-)$
$H \to ZZ^*$	$1.5 \cdot 10^{-3}$	$3.7 \cdot 10^{-3}$	0.31	0.015	0.022

Table 2
Summary of results for the $J^P = 0^+$ versus 1^+ test in the $H \to ZZ^*$ and $H \to WW^*$ channels, as well as their combination. The expected p_0-values for rejecting the $J^P = 0^+$ and 1^+ hypotheses (assuming the alternative hypothesis) are shown in the second and third columns. The fourth and fifth columns show the observed p_0-values, while the $\mathrm{CL_s}$ values for excluding the 1^+ hypothesis are given in the last column.

Channel	1^+ assumed Exp. $p_0(J^P = 0^+)$	0^+ assumed Exp. $p_0(J^P = 1^+)$	Obs. $p_0(J^P = 0^+)$	Obs. $p_0(J^P = 1^+)$	$\mathrm{CL_s}(J^P = 1^+)$
$H \to ZZ^*$	$4.6 \cdot 10^{-3}$	$1.6 \cdot 10^{-3}$	0.55	$1.0 \cdot 10^{-3}$	$2.0 \cdot 10^{-3}$
$H \to WW^*$	0.11	0.08	0.70	0.02	0.08
Combination	$2.7 \cdot 10^{-3}$	$4.7 \cdot 10^{-4}$	0.62	$1.2 \cdot 10^{-4}$	$3.0 \cdot 10^{-4}$

Table 3
Summary of results for the $J^P = 0^+$ versus 1^- test in the $H \to ZZ^*$ and $H \to WW^*$ channels, as well as their combination. The expected p_0-values for rejecting the $J^P = 0^+$ and 1^- hypotheses (assuming the alternative hypothesis) are shown in the second and third columns. The fourth and fifth columns show the observed p_0-values, while the $\mathrm{CL_s}$ values for excluding the 1^- hypothesis are given in the last column.

Channel	1^- assumed Exp. $p_0(J^P = 0^+)$	0^+ assumed Exp. $p_0(J^P = 1^-)$	Obs. $p_0(J^P = 0^+)$	Obs. $p_0(J^P = 1^-)$	$\mathrm{CL_s}(J^P = 1^-)$
$H \to ZZ^*$	$0.9 \cdot 10^{-3}$	$3.8 \cdot 10^{-3}$	0.15	0.051	0.060
$H \to WW^*$	0.06	0.02	0.66	0.006	0.017
Combination	$1.4 \cdot 10^{-3}$	$3.6 \cdot 10^{-4}$	0.33	$1.8 \cdot 10^{-3}$	$2.7 \cdot 10^{-3}$

- The data are compatible with the Standard Model $J^P = 0^+$ quantum numbers for the Higgs boson, whereas all alternative hypotheses studied: $J^P = 0^-, 1^+, 1^-, 2^+$, are excluded at confidence levels above 97.8%.

Cross-sections measurements in the HWW final state

QCD versus electroweak Higgs production

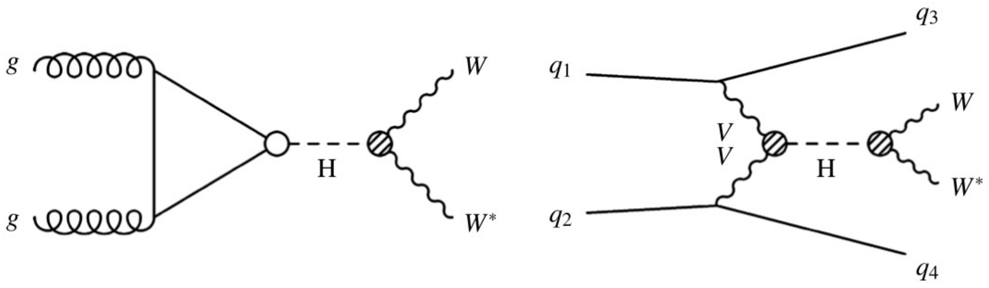

(a) ggF production (b) VBF production

In the leading order no color flow between the forward jets

- VBF features energetic in a forward region in the detector but in opposite directions
  - large rapidity separation $\Delta\eta_{jj}$
  - large m_{jj}
- little hadronic activity in the rapidity region between them – central jet veto (CJV)

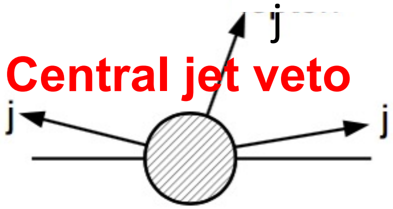

- leptons have intermediate rapidities – outside lepton veto (OLV)

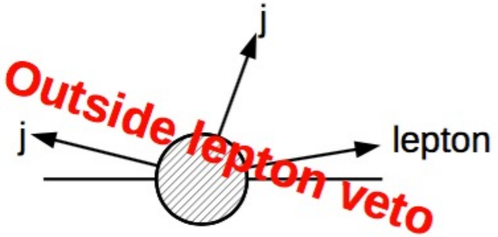

Physics Letters B 789 (2019) 508–529

Measurements of gluon–gluon fusion and vector-boson fusion Higgs boson production cross-sections

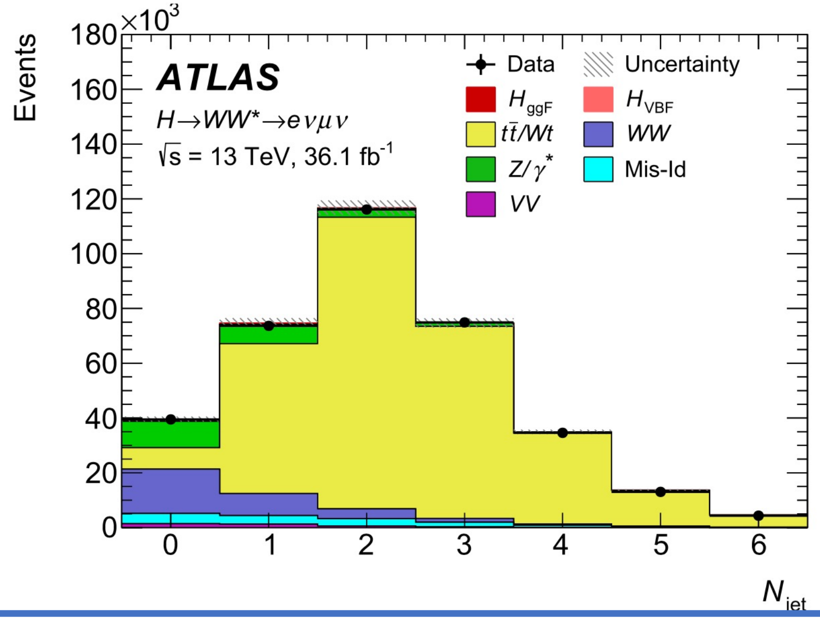

Category	$N_{\text{jet},(p_T>30\text{ GeV})}=0$ ggF	$N_{\text{jet},(p_T>30\text{ GeV})}=1$ ggF	$N_{\text{jet},(p_T>30\text{ GeV})}\geq 2$ VBF
Preselection	Two isolated, different-flavour leptons ($\ell = e, \mu$) with opposite charge $p_T^{\text{lead}} > 22$ GeV, $p_T^{\text{sublead}} > 15$ GeV $m_{\ell\ell} > 10$ GeV $p_T^{\text{miss}} > 20$ GeV		
Background rejection	$N_{b\text{-jet},(p_T>20\text{ GeV})}=0$ $\Delta\phi(\ell\ell, E_T^{\text{miss}}) > \pi/2$ $p_T^{\ell\ell} > 30$ GeV	$\max(m_T^{\ell}) > 50$ GeV $m_{\tau\tau} < m_Z - 25$ GeV	
$H \to WW^* \to e\nu\mu\nu$ topology	$m_{\ell\ell} < 55$ GeV $\Delta\phi_{\ell\ell} < 1.8$		central jet veto outside lepton veto
Discriminant variable BDT input variables	m_T		BDT m_{jj}, Δy_{jj}, $m_{\ell\ell}$, $\Delta\phi_{\ell\ell}$, m_T, $\sum_\ell C_\ell$, $\sum_{\ell,j} m_{\ell j}$, p_T^{tot}

Events are classified into one of three categories based on the number of jets with p_T > 30 GeV

Top, Z/y (and WW) backgrounds estimated from control regions, smaller backgrounds from simulation.

Control regions definitions in the ggf+0/1j and VBF measurements

<table>
<tr><th>CR</th><th>$N_{\text{jet},(p_{\text{T}}>30\ \text{GeV})} = 0$ ggF</th><th>$N_{\text{jet},(p_{\text{T}}>30\ \text{GeV})} = 1$ ggF</th><th>$N_{\text{jet},(p_{\text{T}}>30\ \text{GeV})} \geq 2$ VBF</th></tr>
<tr><td rowspan="3">WW</td><td>$55 < m_{\ell\ell} < 110$ GeV
$\Delta\phi_{\ell\ell} < 2.6$</td><td>$m_{\ell\ell} > 80$ GeV
$|m_{\tau\tau} - m_Z| > 25$ GeV</td><td rowspan="3"></td></tr>
<tr><td colspan="2">$N_{b\text{-jet},(p_{\text{T}}>20\ \text{GeV})} = 0$</td></tr>
<tr><td></td><td>$\max\left(m_{\text{T}}^{\ell}\right) > 50$ GeV</td></tr>
<tr><td rowspan="3">$t\bar{t}/Wt$</td><td>$N_{b\text{-jet},(20\ \text{GeV}<p_{\text{T}}<30\ \text{GeV})} > 0$
$\Delta\phi(\ell\ell, E_{\text{T}}^{\text{miss}}) > \pi/2$
$p_{\text{T}}^{\ell\ell} > 30$ GeV</td><td>$N_{b\text{-jet},(p_{\text{T}}>30\ \text{GeV})} = 1$
$N_{b\text{-jet},(20\ \text{GeV}<p_{\text{T}}<30\ \text{GeV})} = 0$
$\max\left(m_{\text{T}}^{\ell}\right) > 50$ GeV</td><td>$N_{b\text{-jet},(p_{\text{T}}>20\ \text{GeV})} = 1$
central jet veto</td></tr>
<tr><td rowspan="2">$\Delta\phi_{\ell\ell} < 2.8$</td><td colspan="2">$m_{\tau\tau} < m_Z - 25$ GeV</td></tr>
<tr><td></td><td>outside lepton veto</td></tr>
<tr><td rowspan="4">Z/γ^*</td><td colspan="3">$N_{b\text{-jet},(p_{\text{T}}>20\ \text{GeV})} = 0$
$m_{\ell\ell} < 80$ GeV</td></tr>
<tr><td colspan="2">no $p_{\text{T}}^{\text{miss}}$ requirement</td><td>central jet veto</td></tr>
<tr><td></td><td>$\max\left(m_{\text{T}}^{\ell}\right) > 50$ GeV</td><td>outside lepton veto</td></tr>
<tr><td>$\Delta\phi_{\ell\ell} > 2.8$</td><td>$m_{\tau\tau} > m_Z - 25$ GeV</td><td>$|m_{\tau\tau} - m_Z| \leq 25$ GeV</td></tr>
</table>

m_T distribution in ggf+0 and ggf+1j

→ in the control regions for WW, top quark and Z/γ*+jets

↓ combined in the Njet ≤ 1 signal region

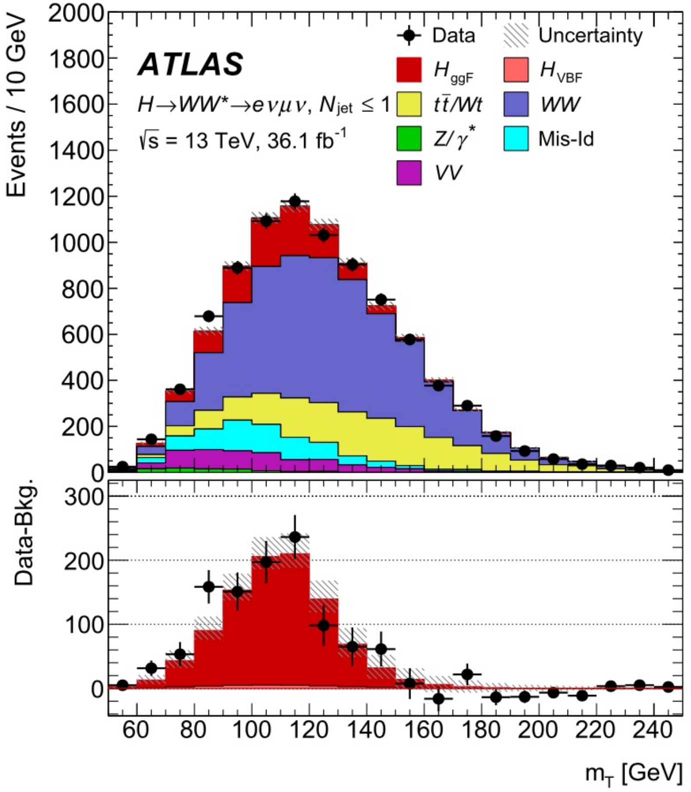

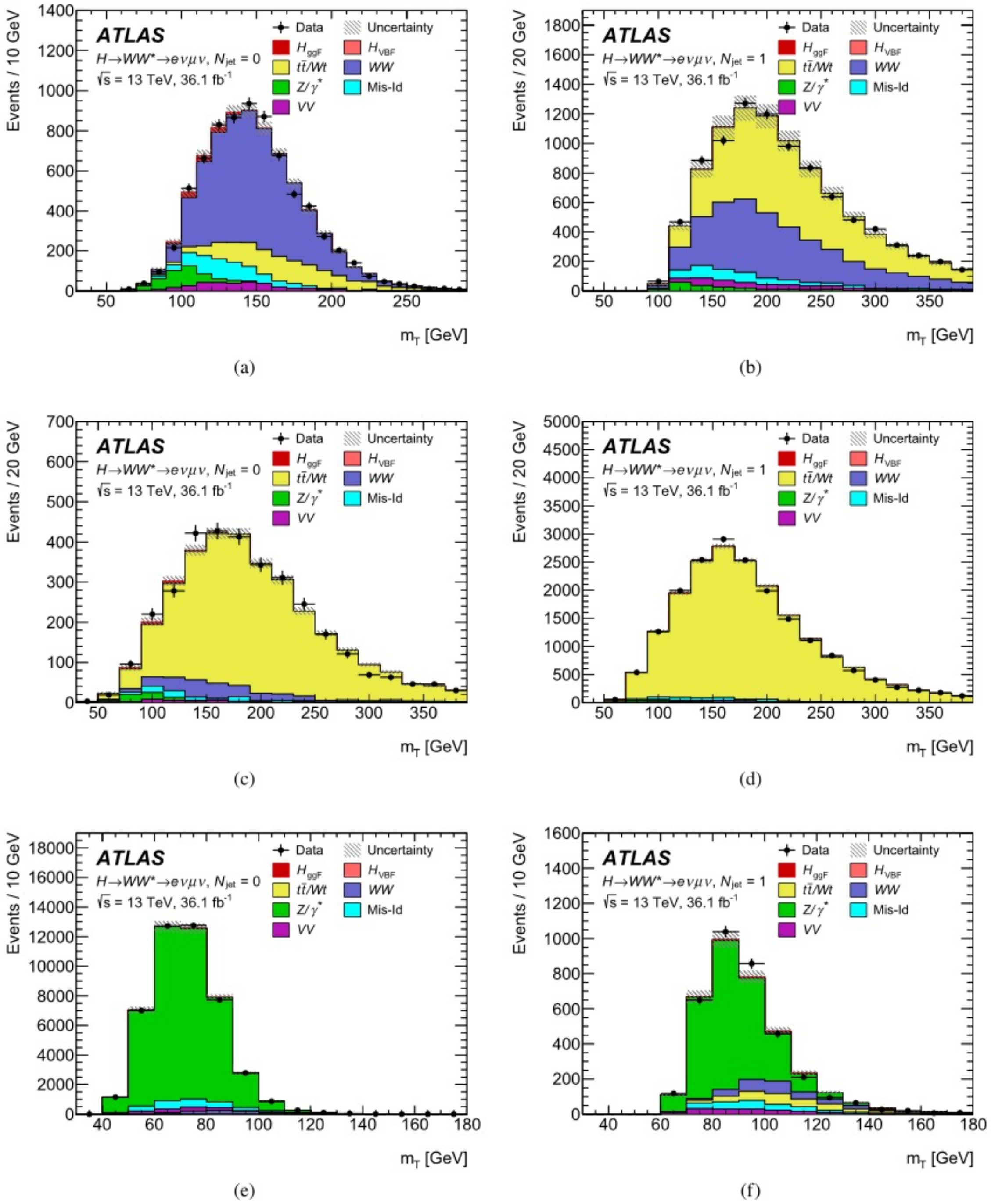

Signal discriminants in VBF

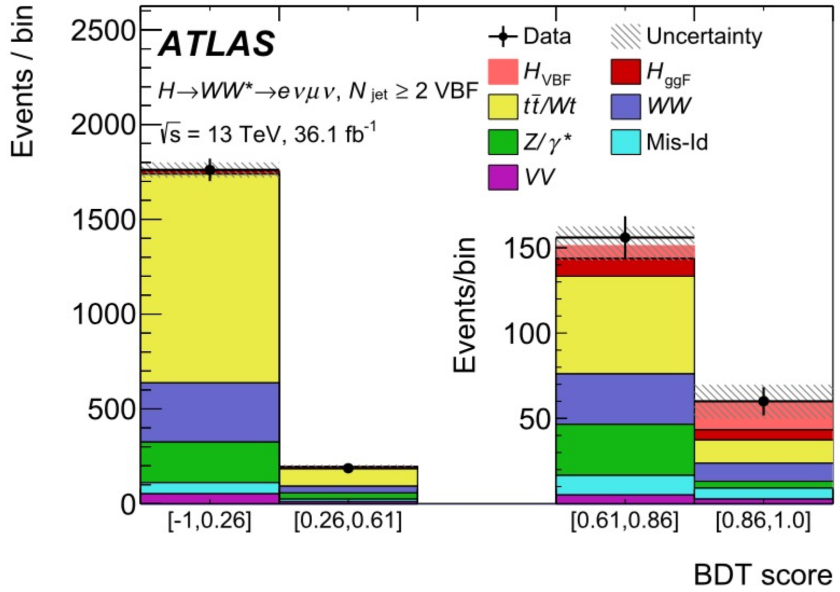

Post-fit BDT score distribution with the signal and the background modelled contributions in the VBF signal region.

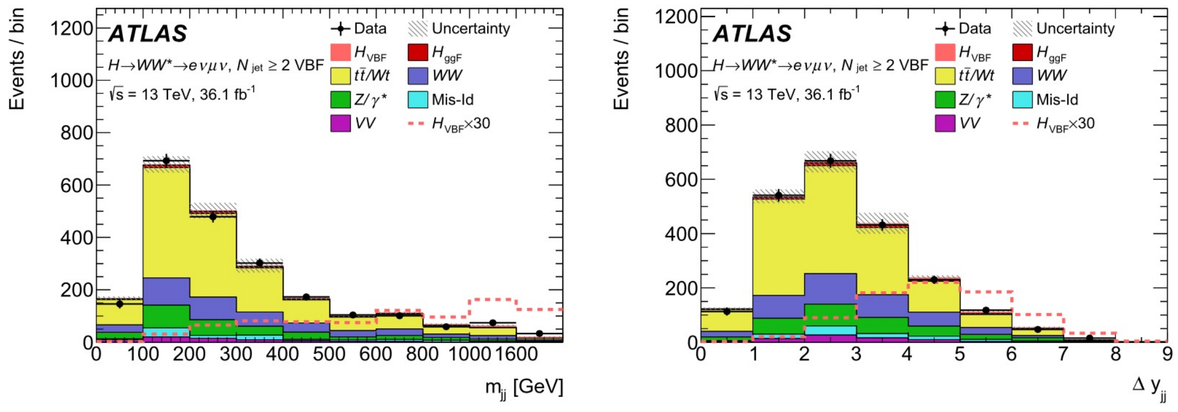

(a) (b)

Post-fit event yields in all signal categories

Process	$N_{jet}=0$ ggF	$N_{jet}=1$ ggF	$N_{jet}\geq 2$ VBF	
			Inclusive	BDT: [0.86, 1.0]
H_{ggF}	639 ± 110	285 ± 51	42 ± 16	6 ± 3
H_{VBF}	7 ± 1	31 ± 2	28 ± 16	16 ± 6
WW	3016 ± 203	1053 ± 206	400 ± 60	11 ± 2
VV	333 ± 38	208 ± 32	70 ± 12	3 ± 1
$t\bar{t}/Wt$	588 ± 130	1397 ± 179	1270 ± 80	14 ± 2
Mis-Id	447 ± 77	234 ± 49	90 ± 30	6 ± 2
Z/γ^*	27 ± 11	76 ± 24	280 ± 40	4 ± 1
Total	5067 ± 80	3296 ± 61	2170 ± 50	60 ± 10
Observed	5089	3264	2164	60

Cross-section measurements

- The measured cross-section times branching fraction values are:

$$\sigma_{\text{ggF}} \cdot \mathcal{B}_{H\to WW^*}$$
$$= 11.4^{+1.2}_{-1.1}(\text{stat.})^{+1.2}_{-1.1}(\text{theo syst.})^{+1.4}_{-1.3}(\text{exp syst.})\ \text{pb}$$
$$= 11.4^{+2.2}_{-2.1}\ \text{pb}$$

$$\sigma_{\text{VBF}} \cdot \mathcal{B}_{H\to WW^*}$$
$$= 0.50^{+0.24}_{-0.22}(\text{stat.}) \pm 0.10(\text{theo syst.})^{+0.12}_{-0.13}(\text{exp syst.})\ \text{pb}$$
$$= 0.50^{+0.29}_{-0.28}\ \text{pb.}$$

- The values predicted in the SM:
  - 10.4 ± 0.6 pb for ggF and
  - 0.81 ± 0.02 pb for VBF.
- The observed (expected) ggF and VBF signals have significances of 6.0 (5.3) and 1.8 (2.6) standard deviations, respectively.

Main sources of systematical uncertainties

Source	$\Delta\sigma_{\text{ggF}} \cdot \mathcal{B}_{H\to WW^*}$ [%]	$\Delta\sigma_{\text{VBF}} \cdot \mathcal{B}_{H\to WW^*}$ [%]
Data statistics	10	46
CR statistics	7	9
MC statistics	6	21
Theoretical uncertainties	10	19
ggF signal	5	13
VBF signal	<1	4
WW	6	12
Top-quark	5	5
Experimental uncertainties	8	9
b-tagging	4	6
Modelling of pile-up	5	2
Jet	2	2
Lepton	3	<1
Misidentified leptons	6	9
Luminosity	3	3
TOTAL	18	57

Constraining Higgs boson properties

arXiv:2109.13808 [hep-ex]

Physics briefing: https://atlas-public.web.cern.ch/updates/briefing/refining-picture-higgs-boson

In a nutshel

Common final state $WW^{*}(\to e\nu\mu\nu)\,jj$, two Higgs production mechanisms

- ggf category
  - CP properties of the top Yukawa coupling and new particles in the gluon fusion loop probed with:

    1D fits to $\kappa_{Agg}/\kappa_{Hgg} \cdot \tan\alpha$ and

    2D fit of CP-even and CP-odd couplings κ_{Hgg} and κ_{Agg} with the mixing angle $\tan\alpha = 1$
  - Measurement of signal strength μ_{ggf+2j}

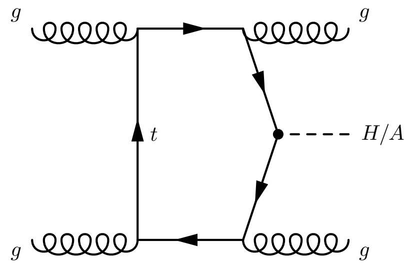

$$\mathcal{L}_0^{\text{loop}} = -\frac{g_{Hgg}}{4}\left(\kappa_{gg}\cos(\alpha)G^a_{\mu\nu}G^{a,\mu\nu} + \kappa_{gg}\sin(\alpha)G^a_{\mu\nu}\tilde{G}^{a,\mu\nu}\right)H$$

CP-even CP-odd

- VBF category
  - Search for BSM physics in Higgs boson individual couplings to longitudinally and transversely polarised W and Z bosons
  - Fits to $a_L = g_{HV_LV_L}/g_{HVV}$ and $a_T = g_{HV_TV_T}/g_{HVV}$ and Pseudo Observables κ_{VV} and ε_{VV}.
  - In the Higgs rest frame only HV_LV_L and HV_TV_T are present.

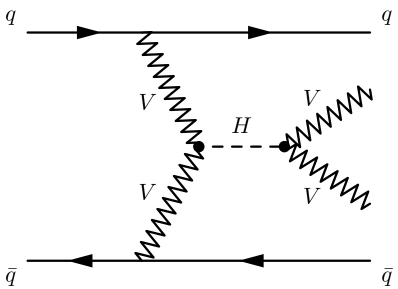

V=W, Z

(following Phys.Rev. D90 (5) (2014) 054023 (2014),arXiv:1404.5951)

Methodology

- **Signal signature:** two (forward) jets, two different flavor opposite sign leptons, no b-quarks
- **Main backgrounds**:
  - double and single top,
  - Z+2jets,
  - WW
  - other dibosons
- **Signal optimisation:** several signal categories, separately for each analysis, using BDTs

- Signal modifications sensitive to the distribution of signed $\Delta\varphi_{jj}$ between jets in the plane perpendicular to the beam axis

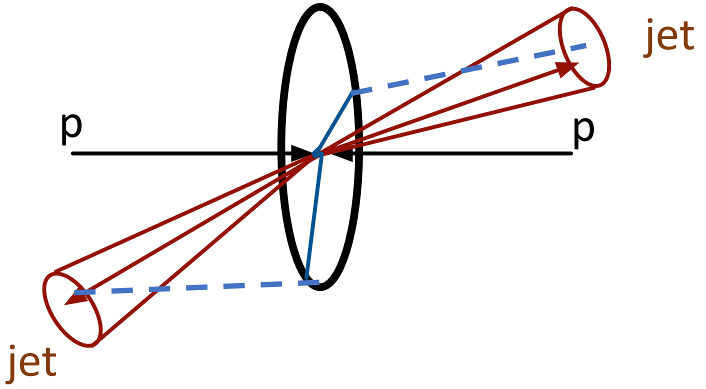

$\Delta\varphi_{jj} = \varphi_{j1} - \varphi_{j2}$ if $\eta_{j1} > \eta_{j2}$, and $\varphi_{jj} = \varphi_{j2} - \varphi_{j1}$ otherwise

Signal and control regions

	ggF + 2 jets	VBF
Preselection	Two isolated, different-flavour leptons ($\ell = e, \mu$) with opposite charge $p_{\mathrm{T}}^{\mathrm{lead}} > 22$ GeV, $p_{\mathrm{T}}^{\mathrm{sublead}} > 15$ GeV $m_{\ell\ell} > 10$ GeV $N_{\mathrm{jet}} \geq 2$	
Background rejection	$N_{b\text{-jet},p_{\mathrm{T}}>20\text{ GeV}} = 0$ $m_{\tau\tau} < 66$ GeV	
	$\Delta R_{jj} > 1.0$ $p_{\mathrm{T},\ell\ell} > 20$ GeV $m_{\ell\ell} < 90$ GeV $m_{\mathrm{T}} < 150$ GeV	central jet veto outside lepton veto
BDT input variables	$m_{\ell\ell}$, m_{T}, $p_{\mathrm{T},\ell\ell}$, $\Delta\phi_{\ell\ell}$ $\min \Delta R(\ell_1, j_i)$, $\min \Delta R(\ell_2, j_i)$	m_{jj}, Δy_{jj}, $m_{\ell\ell}$, m_{T}, $\Delta\phi_{\ell\ell}$ $\sum_{\ell} C_{\ell}$, $\sum_{\ell,j} m_{\ell,j}$, $p_{\mathrm{T}}^{\mathrm{tot}}$

Control region	ggF + 2 jets	VBF
Top CR	$N_{b\text{-jet},(p_{\mathrm{T}}>30\text{ GeV})} = 1$	$N_{b\text{-jet},(p_{\mathrm{T}}>20\text{ GeV})} = 1$
$Z \to \tau\tau$ CR	$\lvert m_{\tau\tau} - m_Z \rvert \leq 25$ GeV	
	$p_{\mathrm{T},\ell\ell}$ requirement is omitted	$m_{\ell\ell} < 80$ GeV
WW CR	$m_{\ell\ell} > 90$ GeV m_{T} requirement is omitted	—

In ggf+2j study the selection requirement placed on p_T^{ll} reduces contributions from the Z + jets background, while the requirements on m_{ll} and m_T decrease the top-quark background.

The VBF signal and control regions are the same as in the cross-section measurement.

Methodology

- To measure properties of the Higgs production vertex the shape of the distribution of $\Delta\Phi_{jj}$ is used. Additionally, in selected fits, $\sigma \cdot Br(H \to WW^*)$ information is employed.

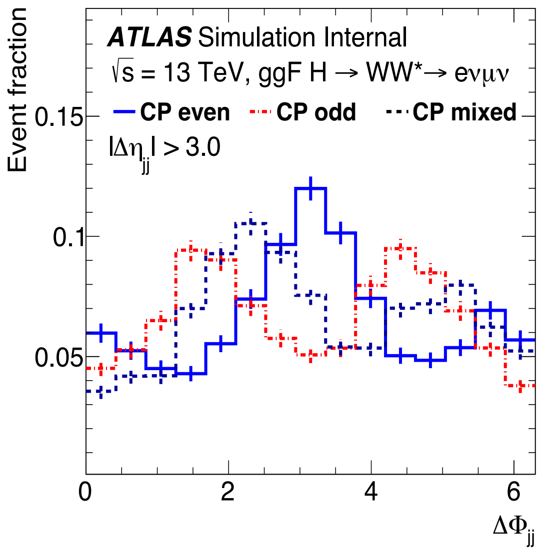

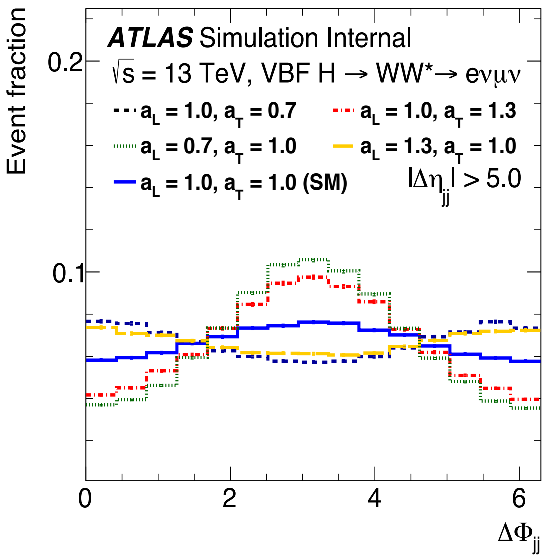

The $\Delta\Phi_{jj}$ distribution in the ggf and VBF signal regions, for selected signals

- Parameter morphing is used to extrapolate from a small set of BSM coupling benchmarks to a large variety of coupling scenarios.

- The final results are obtained by applying a maximum likelihood (ML) procedure individually to each coupling parameter hypothesis, where the background prediction is only affected by changes to nuisance parameters in the minimization.

73.Nucl. Instrum. Meth. A 771 (2015) 39, arXiv:1410.7388 [physics.data-an].

Morphing in a nutshell

Yet another morphing strategy – 'Moment morphing'

- For a Gaussian probability model with linearly changing mean and width, moment morphing of two Gaussian templates is the exact solution
- But also works well on 'difficult' distributions, although interpolation strategy still largely empirical (i.e does not reflect underlying physics principle)

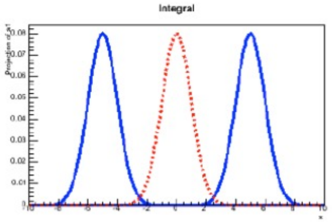

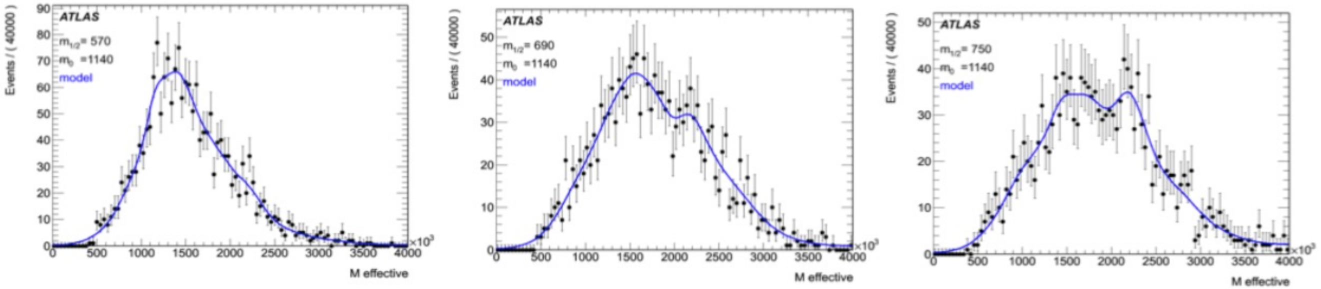

- Calculation of moments of templates is expensive, but just needs to be done once, otherwise very fast (just linear algebra)

- Multi-dimensional interpolation strategies exist
- Moment morphing used for signal interpolation for Run-1 ATLAS CP analysis

Wouter Verkerke, NIKHEF

Improved strategy for interpolation – moment morphing

- Key deficiency of vertical interpolation is that it doesn't account well for shifting distributions

  $T_{out}(x|\alpha) = \alpha^* T_{low}(x)+(1-\alpha)^* T_{high}(x)$

- Alternative strategy is "moment morphing"
- Basic idea is the same, but adjust mean, r.m.s of $T_{low}(x)$,$T_{high}(x)$ through transformation $x \rightarrow x'$ function of α so that mean, r.m.s. of components T(x') match for any α

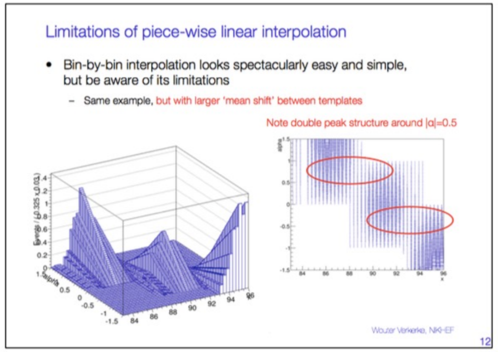
Limitations of piece-wise linear interpolation

- Bin-by-bin interpolation looks spectacularly easy and simple, but be aware of its limitations
  - Same example, but with larger 'mean shift' between templates

Note double peak structure around |α|=0.5

Wouter Verkerke, NIKHEF

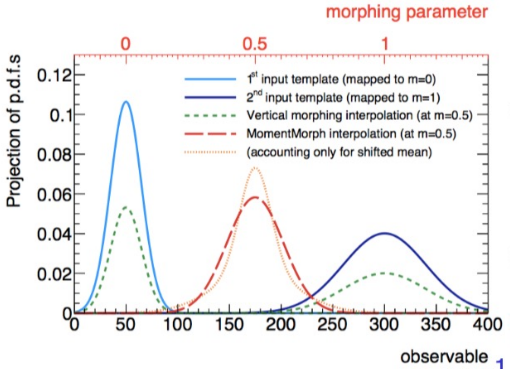

slides from Wouter Verkerke

Effective Lagrangian Morphing

$$T_{\text{out}}(\vec{g}_{\text{target}}) = \sum_i w_i(\vec{g}_{\text{target}}; \vec{g}_i) T_{\text{in}}(\vec{g}_i),$$

discrete input differential distributions (from MC)

observable

SM+BSM couplings

The contribution of each sample T_{in} is weighted by w_i assuming that T ~ $|M|^2$.

using narrow width approximation (Higgs)

$$|\mathcal{M}(\vec{g})|^2 = \underbrace{\left(\sum_{x\in p,s} g_x \mathcal{O}(g_x)\right)^2}_{\text{production}} \cdot \underbrace{\left(\sum_{x\in d,s} g_x \mathcal{O}(g_x)\right)^2}_{\text{decay}},$$

expanding the operators to a 4th degree polynomial in the coupling parameters

$$|\mathcal{M}(\vec{g})|^2 = \sum_{i=1}^{N} X_i \cdot P_i(\vec{g}),$$

g are couplings in the production, decay, or both

$$T_{\text{out}}(\vec{g}) = \sum_{i=1}^{N} \underbrace{\left(\sum_{j=1}^{N} A_{ij} P_j(\vec{g})\right)}_{w_i(\vec{g})} T_{\text{in},i}.$$

$$= \vec{P}(\vec{g}) \cdot A\vec{T},$$

the output distribution should be equal to the input distribution at the respective input parameters

$$A \cdot \left(P_j(\vec{g}_i)\right)_{ij} = \mathbb{1}$$

$$\Leftrightarrow \quad A \cdot G = \mathbb{1}.$$

G depends only on the g's chosen for the input samples, must be non-singular

ggf measurement

The ML fits use as an input the distribution of the signed $\Delta\varphi_{jj}$, divided into 12 categories:

- 3 BDT score intervals: [0.1, 0.4, 0.7, 1.0]
- 4 $|\Delta\eta_{jj}|$ intervals: [0.0, 1.0, 2.0, 3.0, ∞],

Four different fits are performed:

- The signal strength parameter $\mu_{ggF+2jets}$ defined as the ratio of the measured signal yield to that predicted by the SM.
- In order to constrain BSM effects in the effective Higgs–gluon coupling, tan(α) is scanned:
  - The normalisation of the signal process is unconstrained (a shape only fit)
  - The signal normalisation is constrained to the model predictions (a shape and rate fit)
- A simultaneous fit of the coupling-strength scale factors κgg cos(α) and κgg sin(α) is performed. This study exploits both shape and rate information.

Results

- The mixing angle for CP-even and CP-odd contributions to the effective Higgs– gluon interaction is determined to be tan(α) = 0.0 ± 0.4(stat.) ± 0.3(syst.) using both shape and rate information, shape only fits not yet sensitive.

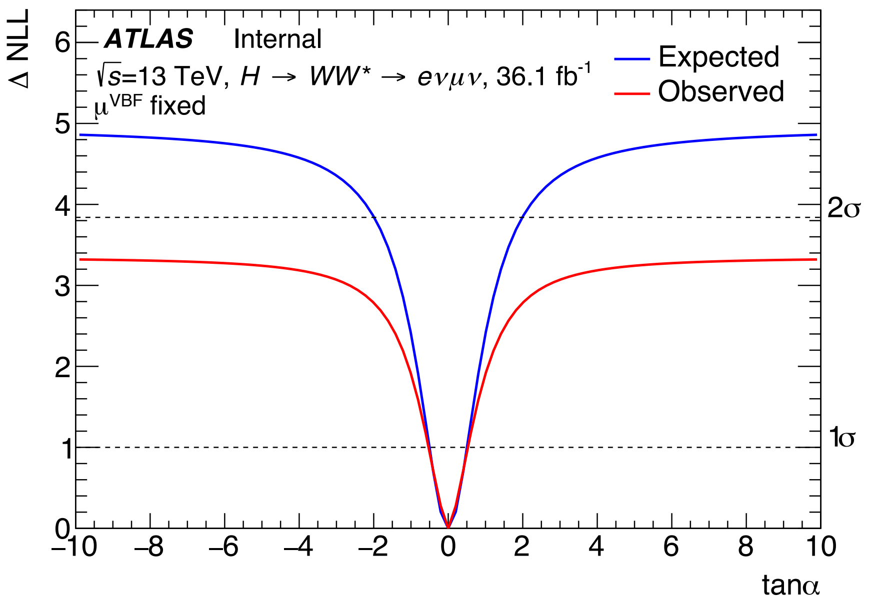

- 68% and 95% CL two-dimensional likelihood contours of the CP-even and CP-odd coupling parameters

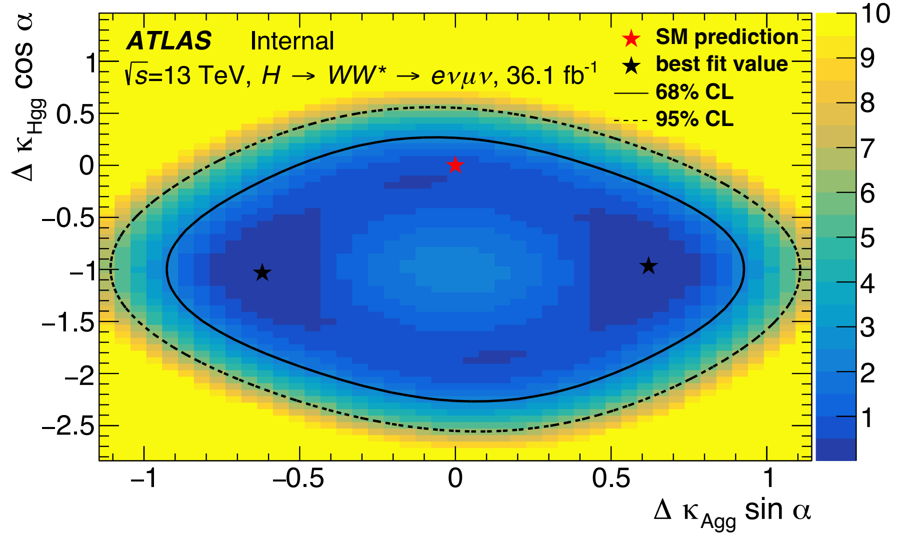

- Measured the signal strength

$$\mu_{ggF+2j} = 0.5 \pm 0.4(\text{stat.})\ _{-0.6}^{+0.7}\ (\text{syst.})$$

VBF measurement

Are the Higgs HVV couplings really scalar?

At infinitely large momenta the transverse parts of V bosons correspond to the “proper” gauge bosons, whereas the longitudinal parts arise from the “eaten” Goldstone bosons.

VBF H→ WW as a part of WW scattering

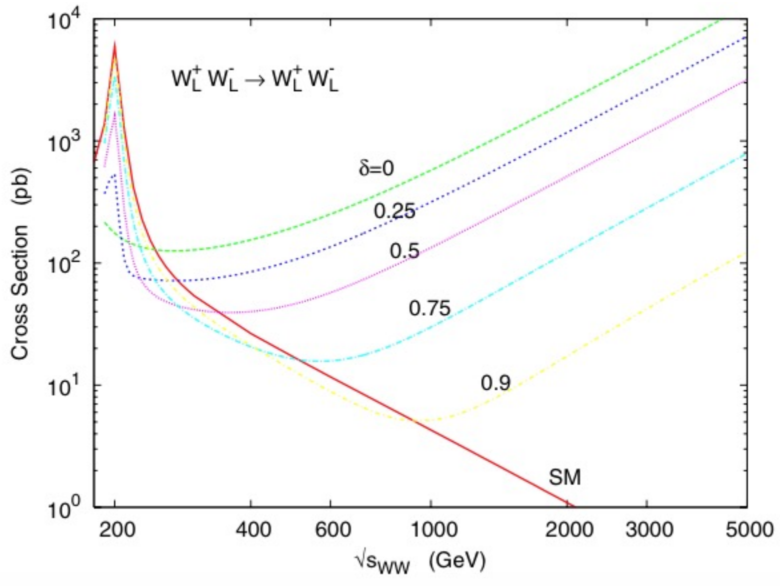

PHYS.REV.D 78, 051701(R) (2008)

WW scattering

- The Higgs mechanism introduces masses of gauge bosons and their longitudinal polarisations

$$e^{\mu}_{\pm} = \frac{1}{\sqrt{2}}(0,1,\pm i,0), \quad e^{\mu}_{L} = \frac{\sqrt{s}}{2M_W}(\beta,0,0,1)$$

- As a consequence $W_L W_L$ scattering amplitude diverges with center of mass energy
- O(s) divergence

subtracted by Higgs diagrams if $g_{HVV}=g_V\, m_{VV}$ (gauge invariance requirement)

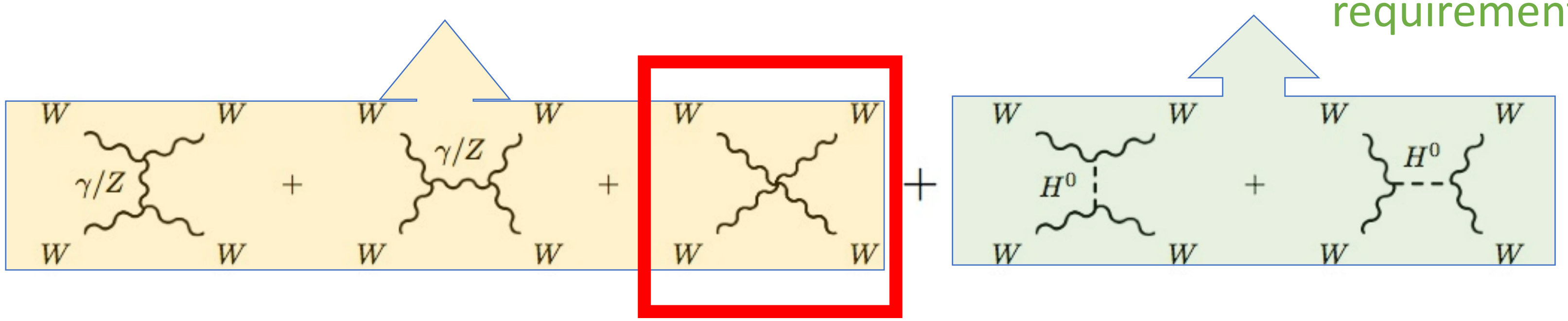

- Test the SM EW symmetry breaking.
- In the SM there is no distinction between coupling strengths of HV_LV_L and HV_TV_T interactions.
- At infinitely large momenta the transverse parts of V bosons correspond to the “proper” gauge bosons, whereas the longitudinal parts arise from the eaten Goldstone bosons.
- HVV couplings are sensitive to new physics in EWSB: extended Higs sectors, Higgs as a composite pseudo-Goldstone boson (SILH, MCHM), ...

Kinematical effects of coupling modifications

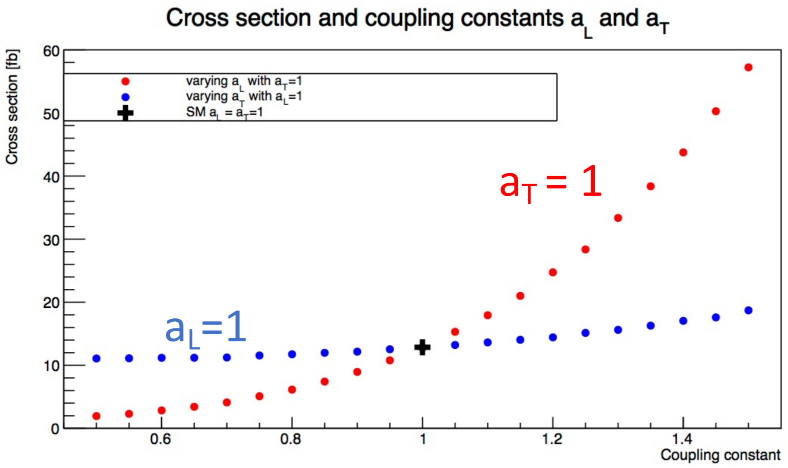

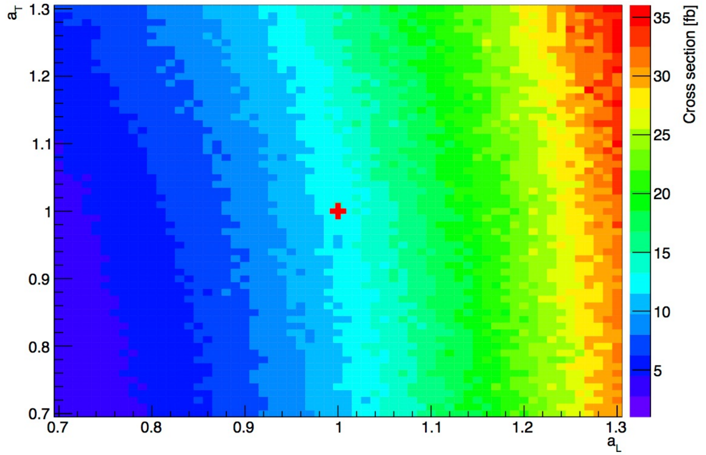

- Total rates (σ_{VBF} x Br(h->WW)) more sensitive to a_L as VBF is dominated by longitudinal W scattering at high energies
- The most discriminating distribution is

  signed $\Delta\varphi_{jj}$

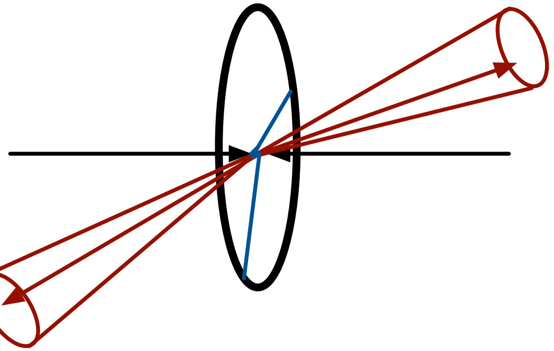

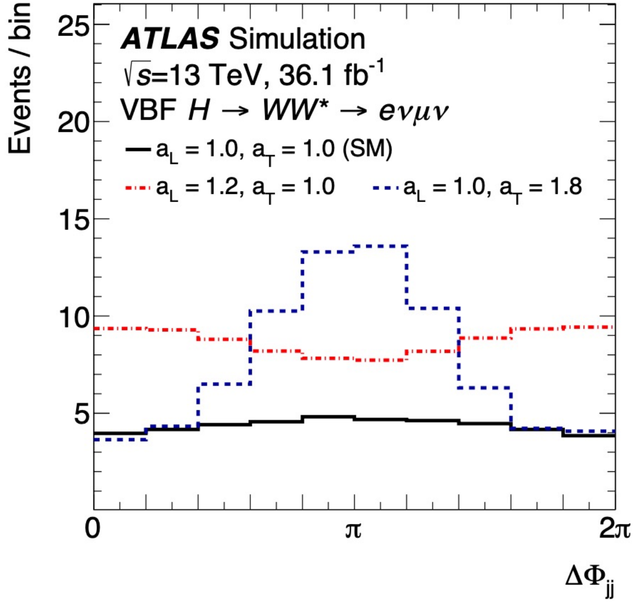

Mapping to Pseudo-Observables

Eur. Phys. J. C 75 (2015) 128, arXiv:1412.6038 [hep-ph]

Signal paraletrised using (a_L, a_T) couplings scale factors is not Lorentz invariant.

Approximate(*) mapping to Pseudo Observables:

$$\boxed{\begin{aligned} a_L &= \kappa_{VV} + \Delta_L(q_1, q_2)\epsilon_{VV}, \quad a_T = \kappa_{VV} + \Delta_T(q_1, q_2)\epsilon_{VV}. \\ \kappa_{VV} &= a_\mathrm{L} - \Delta_\mathrm{L}(q_1, q_2)\varepsilon_{VV}, \quad \varepsilon_{VV} = \frac{a_\mathrm{T} - a_\mathrm{L}}{\Delta_\mathrm{T}(q_1, q_2) - \Delta_\mathrm{L}(q_1, q_2)} \end{aligned}}$$

where

$$\Delta_\mathrm{L} = \frac{m_H^2}{2m_W^2} \frac{4q_1^2 q_2^2}{m_H^2(m_H^2 - q_1^2 - q_2^2)}, \quad \Delta_\mathrm{T} = \frac{m_H^2}{2m_W^2} \frac{m_H^2 - q_1^2 - q_2^2}{m_H^2}.$$

From MG5 simulation the mean values of formfactors for incoming bosons (generator level cuts) are:

Δ_L(q$_1$, q$_2$) =0 and Δ_T(q$_1$, q$_2$)= 2 $\frac{{m_h}^2}{2{m_V}^2}$

$$\boxed{\kappa_{VV} = a_L, \quad \varepsilon_{VV} = 0.5\,(a_T - a_L),}$$

In the SM: on-shell coupling κ_{VV}= 1, off-shell coupling ε_{VV} = 0

(*) assuming custodial symmetry, no new physics in the boson–fermion couplings Wff and Zff , and a CP-even Higgs boson with CP-conserving HVV interactions.

VBF measurement

- Object definitions, signal selection and background estimation the same as in the ggf+VBF analysis.
- Input distribution consists of 4 BDT bins, each containing 10 $\Delta\varphi_{\mathrm{jj}}$ bins
- Simultaneous fit of:
  - $\Delta\varphi_{\mathrm{jj}}$ in 4 BDT bins in the SR
  - One bin (normalisation) fit in CRs
- Results from fits in (a_L, a_T) and ($\boldsymbol{\kappa}_{\mathrm{VV}}$, $\boldsymbol{\varepsilon}_{\mathrm{VV}}$) parametrisations, where the other parameter is fixed or profiled

Results

Type	Expected	Observed
a_T shape-only fit (a_L = 1)	$1.0 \pm 0.5(\text{stat.})^{+0.3}_{-0.4}(\text{syst.})$	$1.3^{+0.8}_{-0.4}(\text{stat.})^{+0.3}_{-0.2}(\text{syst.})$
a_L shape + rate fit (a_T = 1)	$1.00^{+0.08}_{-0.10}(\text{stat.})^{+0.07}_{-0.13}(\text{syst.})$	$0.90^{+0.09}_{-0.13}(\text{stat.})^{+0.08}_{-0.18}(\text{syst.})$
a_T shape + rate fit (a_L = 1)	$1.00^{+0.36}_{-0.49}(\text{stat.})^{+0.19}_{-0.27}(\text{syst.})$	$1.19^{+0.27}_{-0.32}(\text{stat.})^{+0.12}_{-0.14}(\text{syst.})$
a_L shape + rate fit (a_T profiled)	$1.00^{+0.08}_{-0.10}(\text{stat.})^{+0.08}_{-0.13}(\text{syst.})$	$0.91^{+0.10}_{-0.18}(\text{stat.})^{+0.09}_{-0.17}(\text{syst.})$
a_T shape + rate fit (a_L profiled)	$1.0^{+0.4}_{-0.5}(\text{stat.})^{+0.2}_{-0.4}(\text{syst.})$	$1.2 \pm 0.4(\text{stat.})^{+0.2}_{-0.3}(\text{syst.})$

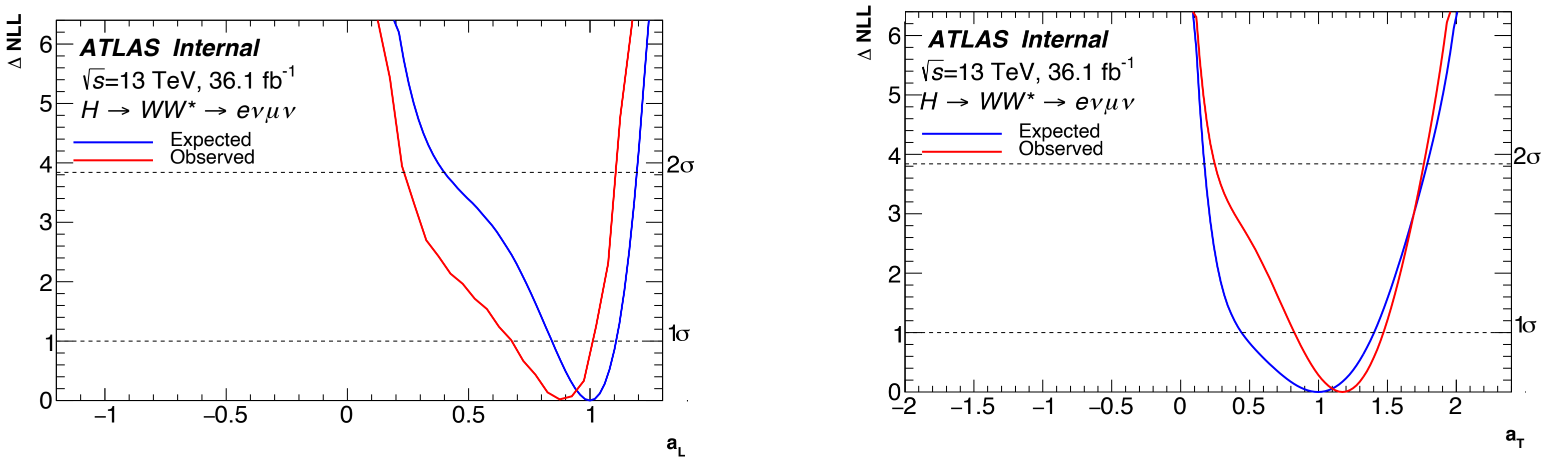

Results

Type	Expected	Observed
ε_{VV} shape-only fit ($\kappa_{VV}=1$)	$0.00^{+0.23}_{-0.25}$(stat.)$^{+0.14}_{-0.17}$(syst.)	$0.14^{+0.39}_{-0.22}$(stat.)$^{+0.16}_{-0.12}$(syst.)
κ_{VV} shape + rate fit ($\varepsilon_{VV}=0$)	$1.00^{+0.08}_{-0.10}$(stat.)$^{+0.08}_{-0.13}$(syst.)	$0.91^{+0.09}_{-0.12}$(stat.)$^{+0.09}_{-0.18}$(syst.)
ε_{VV} shape + rate fit ($\kappa_{VV}=1$)	$0.00^{+0.18}_{-0.24}$(stat.)$^{+0.08}_{-0.13}$(syst.)	$0.09^{+0.13}_{-0.16}$(stat.)$^{+0.06}_{-0.07}$(syst.)
κ_{VV} shape + rate fit (ε_{VV} profiled)	$1.00^{+0.08}_{-0.10}$(stat.)$^{+0.08}_{-0.13}$(syst.)	$0.91^{+0.10}_{-0.18}$(stat.)$^{+0.09}_{-0.17}$(syst.)
ε_{VV} shape + rate fit (κ_{VV} profiled)	$0.00^{+0.22}_{-0.24}$(stat.)$^{+0.11}_{-0.15}$(syst.)	$0.13^{+0.28}_{-0.20}$(stat.)$^{+0.08}_{-0.10}$(syst.)

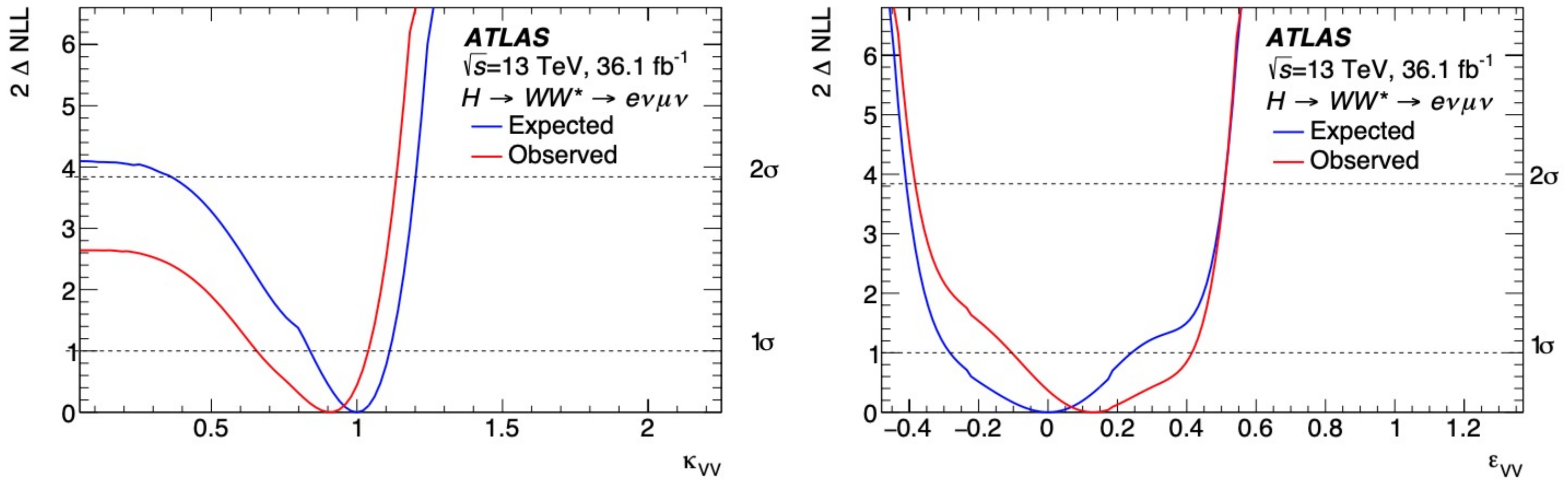

(a) κ_{VV} shape+rate fit with profiled ε_{VV} (b) ε_{VV} shape+rate fit with profiled κ_{VV}

Conclusions and outlook

- With more data increased sensitivity to Higgs boson processes, new processes are being explored.
- Improving measurements of Higgs boson cross-sections and branching ratios, as well as constraints on its couplings.
- New developments in experimental techniques and statistical analysis
- On-going discussions with theorists on comunicating experimental results in the best way to test theoretical predictions
  - constraints on sets of effective field theory operators are underway
  - increasing role of differential measurements (the framework of simplified template cross-sections)

- Combinations of various final states as well as Higgs and electroweak processes are vital in maximising research potential of the LHC experiments.

Backup slides

Morphing likelihood ratios

The minimisation condition of a likelihood fit has a form

$$\widehat{\vec{g}}(T_d) = \arg\min_{\vec{g}} -2\ln P\left(T_d \mid \mu = \sum_{i=1}^{N}\left(\sum_{j=1}^{N} A_{ij} P_j(\vec{g})\right) T_{\text{in},i}\right).$$

so that only the polynomials $P_j(g)$ need to be recalculated during the minimisation process, while the non-trivial quantities stay fixed.

Calculation of moments of input templates expensive, but done only once in the calculation.

The error propagation of statistical uncertainties to the output T_{out} occurs only via linear combinations.

- Morphing only requires that any differential cross section can be expressed as polynomial in BSM couplings
- Method can be used on any generator that allows one to vary input couplings
- Works on truth and reco-level distributions
- Independent of physics process
- Works on distributions and cross sections
- Implemented in the *RooLagrangianMorphing* class in RooFit.

Morphing model prediction is a weighted sum of templates.

- Need to take care that relevant regions of parameters do not end up being modeled by low-statistics samples with large scale factors.
- Choice of input samples is important (in practice done by trial and error)

Coupling modifiers and dim-6 EFT operators

$$\mathcal{L}_{SM} = (\mathbf{D}_\mu\phi)^\dagger \mathbf{D}^\mu \phi$$
$$\mathcal{L}_{\phi W} = -\frac{g^2 F_{\phi W}}{4}\left(\phi^\dagger\phi - \frac{v^2}{2}\right) \mathrm{tr}\left[\mathbf{W}_{\mu\nu}\mathbf{W}^{\mu\nu}\right],$$
$$\mathcal{L}_{\phi} = F_{HD}\left(\phi^\dagger\phi - \frac{v^2}{2}\right)\left((\mathbf{D}_\mu\phi)^\dagger \mathbf{D}^\mu \phi\right).$$

$$a_T = 1 + \frac{v^2 F_\phi}{2} + F_{\phi W} q_1 \cdot q_2 ,$$
$$a_L = 1 + \frac{v^2 F_\phi}{2} + F_{\phi W} \frac{q_1^2 q_2^2}{q_1 \cdot q_2} .$$

Mapping between (a_L and a_T) and EFT operators momentum dependent. EFT kinematics can be reproduced fitting a_L and a_T (see 1404.5951)
Independent variations in (a_L and a_T) not possible in the dimension-6 set of EFT operators

Methodology

To measure properties of the Higgs production vertex the shape of the distribution of the azimuthal angle between two tagging jets $\Delta\Phi_{jj}$ is used. Additionally, in selected fits, $\sigma \cdot Br(H \rightarrow WW^*)$ information is employed.

Parameter morphing is used to extrapolate from a small set of BSM coupling benchmarks to a large variety of coupling scenarios.

The final results are obtained by applying a maximum likelihood procedure individually to each coupling parameter hypothesis, where the background prediction is only affected by changes to nuisance parameters in the minimization.

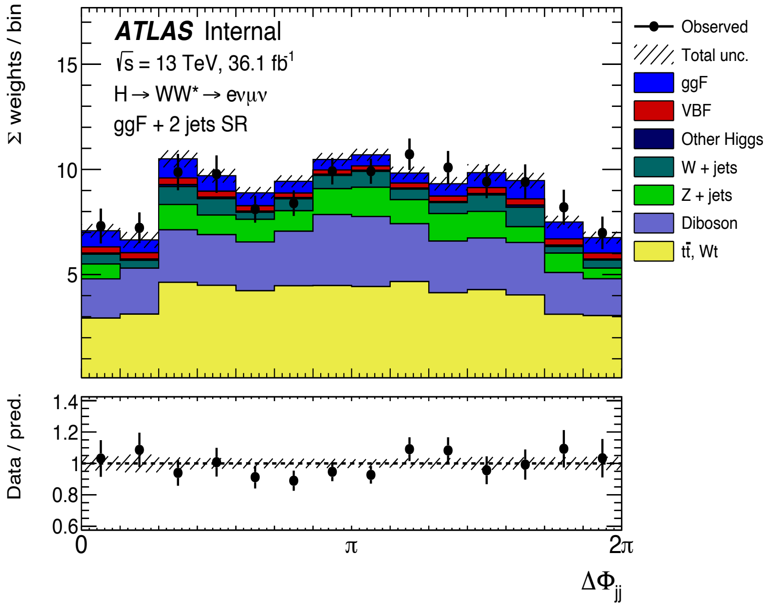

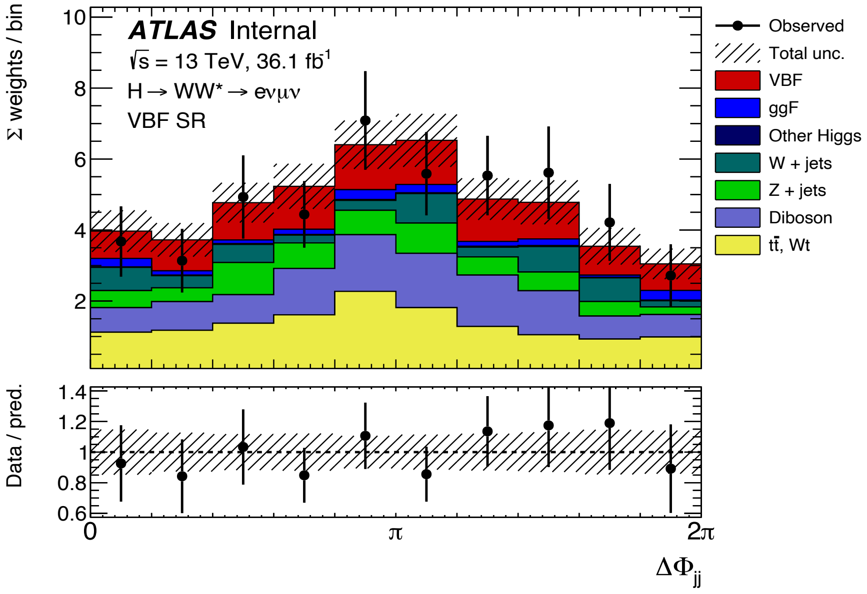

The weighted $\Delta\Phi_{jj}$ distribution in the ggf and VBF signal regions, with signal and background yields fixed from the fits.

Main sources of uncertainties in the VBF Higgs properties analysis

Source	$\Delta\kappa_{VV}$
Total data statistical uncertainty	0.11
SR data statistical uncertainty	0.10
CR data statistical uncertainty	0.019
MC statistical uncertainty	0.035
Total systematic uncertainty	0.12
Theoretical uncertainty	0.10
Top-quark bkg.	0.072
WW bkg.	0.062
ggF bkg.	0.033
Z/γ^* bkg.	0.017
VBF signal	0.019
Experimental uncertainty	0.050
Jet	0.026
b-tagging	0.014
Luminosity	0.011
Misidentified leptons	0.007
Total	0.17

(a) κ_{VV} fit, $\varepsilon_{VV} = 0$

Source	$\Delta\varepsilon_{VV}$
Total data statistical uncertainty	0.14
SR data statistical uncertainty	0.14
CR data statistical uncertainty	0.011
MC statistical uncertainty	0.036
Total systematic uncertainty	0.056
Theoretical uncertainty	0.050
Top-quark bkg.	0.039
WW bkg.	0.036
ggF bkg.	0.013
Z/γ^* bkg.	0.012
VBF signal	0.010
Experimental uncertainty	0.024
Modelling of pile-up	0.022
Jet	0.018
Misidentified leptons	0.010
b-tagging	0.010
Total	0.16

(b) ε_{VV} fit, $\kappa_{VV} = 1$